

1 **Deciphering T-wave Morphologies on ECGs: The Simplified Egg and** 2 **Changing Yolk Model and the Importance of the QTp Interval**

3 Kieran Stone^{1, †} PhD, Dr Arvind Mistry^{1, †} BSc (Hons), MBBS, DCH, DFFP, MBA, Daniel
4 Cyrus ² BSc, Dr John Cannon³ BSc (Hons) MBBS, DRCOG, DFFP, DTher, FRCGP, FRSA,
5 AFHEA, Ignacy Mokrzecki¹ BSc and Faisal I Rezwan^{1,*} PhD.

- 6 1. Department of Computer Science, Aberystwyth University, Wales, SY23 3DB, UK.
- 7 2. University of Surrey, Stag Hill, University Campus, Guildford, GU2 7XH, UK.
- 8 3. University of Suffolk, Waterfront Building, 19 Neptune Quay, Ipswich, IP4 1QJ, UK.

9 * Address reprint requests and correspondence: Dr. Faisal I. Rezwan, Department of
10 Computer Science, Aberystwyth University, Wales, SY23 3DB, United Kingdom. Email
11 address: f.rezwan@aber.ac.uk.

12 † Authors contributed equally to this work.

13

14

15

16

17 **Abstract**

18 The Electrocardiogram (ECG) serves as an integral tool in the diagnosis and
19 management of a variety of cardiac diseases. It visualises electrical activity in the heart,
20 offering insights into several cardiac processes, including ventricular repolarisation. The
21 morphology of the T-wave observed on ECGs during this repolarisation phase varies and
22 can be peaked, flat, inverted, or biphasic, each representing different cardiac
23 conditions. Despite their prevalence, the interpretation of these patterns remains
24 challenging. Therefore, we proposed the Simplified Egg and Changing Yolk Model, a
25 novel idea to aid in the understanding of these T-wave morphologies in ECGs.

26 The proposed Simplified Egg and Changing Yolk Model was developed through an
27 analysis of various T-wave morphologies and their corresponding clinical implications.
28 The model was further designed to conceptualise the ST interval and the T-wave as a
29 single unit, contributing to a simplified yet comprehensive understanding of ventricular
30 repolarisation. In this context, the 'Q-wave start to T-wave peak interval' (QTp) was
31 compared to the more commonly used 'corrected QT-interval' (QTc) for assessing the
32 risk of arrhythmia and the effects of medication that prolong the QT-interval.

33 The Simplified Egg and Changing Yolk Model could effectively explain and interpret the
34 variation of ECG patterns associated with ventricular repolarisation. It provided insight
35 into the relevance of deflections seen during this phase. Importantly, the model
36 identified QTp as a more reliable measure than QTc for assessing arrhythmia risk and
37 evaluating medication impacts on the QT-interval.

38 Our model offers a significant enhancement to the understanding of ventricular
39 repolarisation and its manifestation on ECGs. By emphasising the superiority of QTp

40 over QTc in clinical assessment, this model can have significant impact in clinical
41 practice.

42 **Keywords:** Electrocardiogram (ECG), Ventricular repolarisation, T-wave morphology,
43 QTp interval, Cardiac arrhythmia, QT interval, QTc interval, ECG interpretation, Cardiac
44 diagnostic models, Clinical cardiology

45

46

47

48

49

50

51

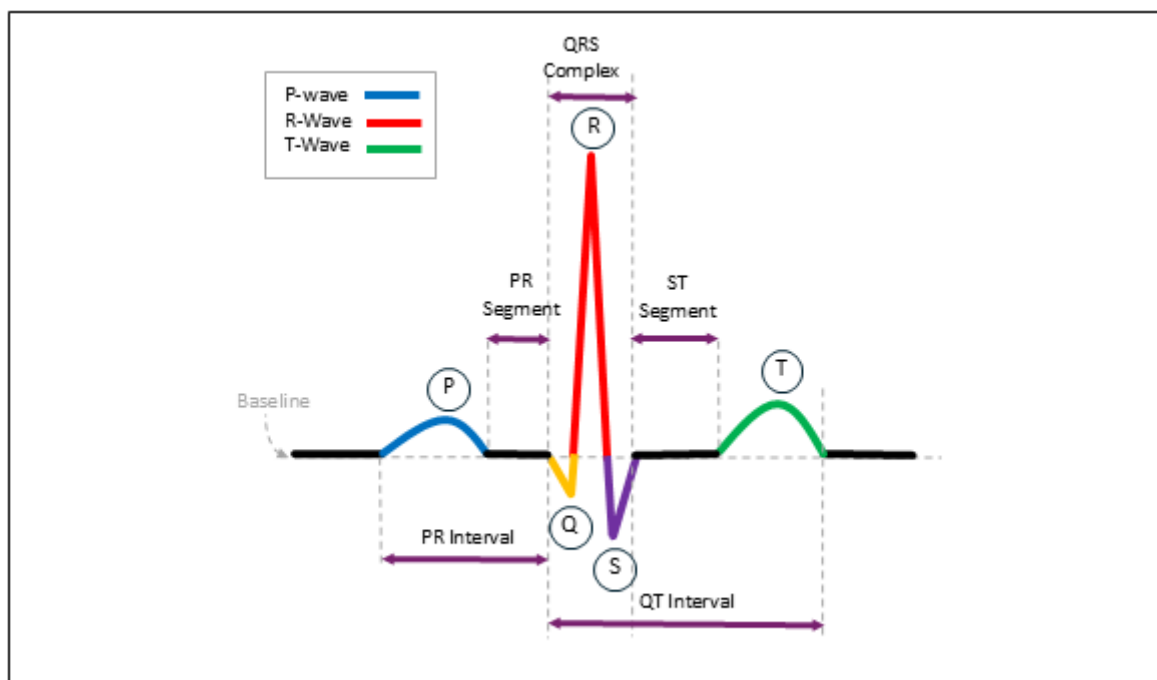
52

53

54

55 Introduction

56 Electrocardiogram (ECG) signals provide significant information about a patient's heart
57 processes and are widely used to investigate both normal and pathological conditions
58 of the heart¹. These signals display the time evolution of the heart's electrical activity for
59 each heartbeat in the cardiac cycle, typically consisting of distinct depolarisation and
60 repolarisation patterns². These electrical activities in each cardiac cycle are detected by
61 an ECG device and translates them into a graphical representation to identify anomalies
62 in heart rhythm or any changes in heart morphology^{3,4}. Any deviations in ECG traces
63 from the 'normal pattern' (shown in Figure 1) are empirically interpreted by clinicians as
64 'ECG abnormalities'.



65
66 **Figure 1: The classic ECG wave.** The classic ECG wave illustrates the essential components of cardiac
67 electrical activity, including the P-wave, QRS complex, and T-wave, as well as their respective intervals.

68 This knowledge has evolved over many years, with clinicians matching ECG patterns to
69 pathological changes in the heart through experience. While this approach has been

70 effective, it often lacks sufficient explanations for why certain patterns appear as they
71 do, leading to the propagation of concepts without fully questioning the underlying
72 reasons for the formation of these ECG traces.

73 Ventricular repolarisation as reflected in various T-wave morphologies on ECG traces, is
74 a key aspect clinicians use to assess heart conditions. For instance, changes in the ST
75 segment are crucial indicators of ischemia or infarct⁵. Despite their diagnostic
76 importance, the underlying mechanisms causing ST elevation and ST depression
77 remain unclear, with no definitive explanation provided for these phenomena⁶.

78 Additionally, the absence of a definitive explanation for the typical ‘hump’ shape of the
79 T-wave on an ECG, coupled with the unclear mechanisms behind various atypical T-
80 wave morphologies such as peaked, inverted, flattened, or biphasic patterns, are
81 particularly noteworthy^{7,8}.

82 Beyond the limited understanding of the mechanisms behind various atypical T-wave
83 morphologies, the QT interval is a crucial measurement on ECGs. Essentially, the QT
84 interval reflects the time required for the heart’s ventricles to contract and then relax in
85 preparation for the next heartbeat. This is crucial in evaluating heart function, as an
86 abnormal duration may indicate various cardiac conditions, including arrhythmias⁹. A
87 prolonged QT interval is associated with an increased risk of developing a potentially
88 life-threatening arrhythmia known as Torsades de Pointes, while a shortened QT interval
89 may also be linked to specific cardiac disorders^{10,11}.

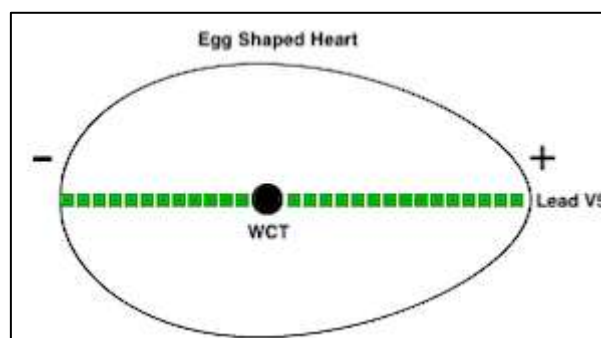
90 It is also noteworthy that the QT interval is influenced by heart rate¹². Consequently, it is
91 frequently corrected for the patient’s heart rate using different formulae (e.g. Bazett’s or
92 Fridericia’s formulae), resulting in the corrected QT interval (QTc)¹³. However, several

93 issues are associated with the current QTc interval when comparing cases of heart rate
94 variability (for more details see Supplementary Material section 1).

95 This study explores ECG electrophysiology by focusing on its link to Wilson’s Central
96 Terminal (WCT) and the origins of ECG deflections. We present a novel approach, the
97 "Simplified Egg and Changing Yolk Model", to clarify the ventricular repolarisation
98 process seen in the T-wave. This model explains common T-wave abnormalities,
99 enhancing the accuracy and effectiveness of QT interval analysis.

100 **The Simplified Egg and Changing Yolk Model**

101 The “Simplified Egg and Changing Yolk Model” views the ventricular repolarisation
102 process as occurring within a mass of heart muscle, simplified into an ‘egg’ shape. This
103 shape influences the electrical deflection detected by ECG leads, depending on
104 electrode position. In this example the green line represents the vector of lead V5,
105 passing through the egg’s long axis. Signals detected to the right of the WCT for lead V5
106 register as positive, while those on the left register as negative. The resulting ECG trace
107 is the net outcome of these positive and negative signals over time (see Figure 2)¹⁴.



108
109 **Figure 2: Representation of the heart in the Simplified Egg and Changing Yolk Model.** This figure
110 depicts the heart as an egg-shaped 3D object, with the WCT at its centre.

111 **Normal repolarisation sequence as explained by the model**

112 In the Simplified Egg and Changing Yolk Model, the repolarisation signal expands from
113 the WCT to the edges until the entire muscle mass has completed repolarisation. The
114 expanding ‘yolk’ can be likened to ripples emanating from a stone dropped into still
115 water, spreading out from the centre (WCT) in all directions but extending further on one
116 side due to the asymmetrical egg shape. The model states that an ECG lead detects the
117 one-dimensional repolarisation signal based on its vector through the egg shape.
118 Signals moving in front of the WCT point produce a positive deflection, while those
119 moving away cause a negative deflection¹⁵. The net result of these signals is registered
120 on the ECG trace over time for that lead.

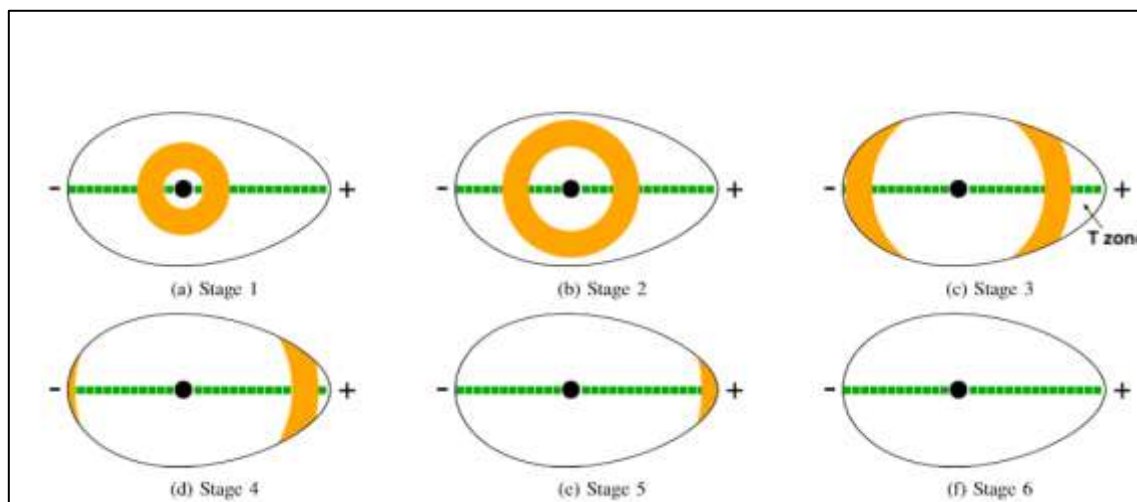
121 The sequence of the repolarising signal expanding out from the WCT to the outer
122 boundaries of the egg shape is shown in Figure 3. The lead V5 vector is shown as a
123 green line pointing into the egg through the WCT and in this example is looking from the
124 right side of the egg shape. As the signal expands (shown in orange in the diagram) the
125 net result from the positive and negative sides of the lead register as deflections
126 (positive or negative) depending on which side has the greater signal amplitude. For a
127 specified lead, this is represented as the following formula:

$$128 \quad LD_T = S_T - S_A$$

129 Here, LD_T is the deflection for a specified lead at time T , S_T represents the signal
130 components moving towards the lead and S_A represents the signal components moving
131 away from the lead at a given time.

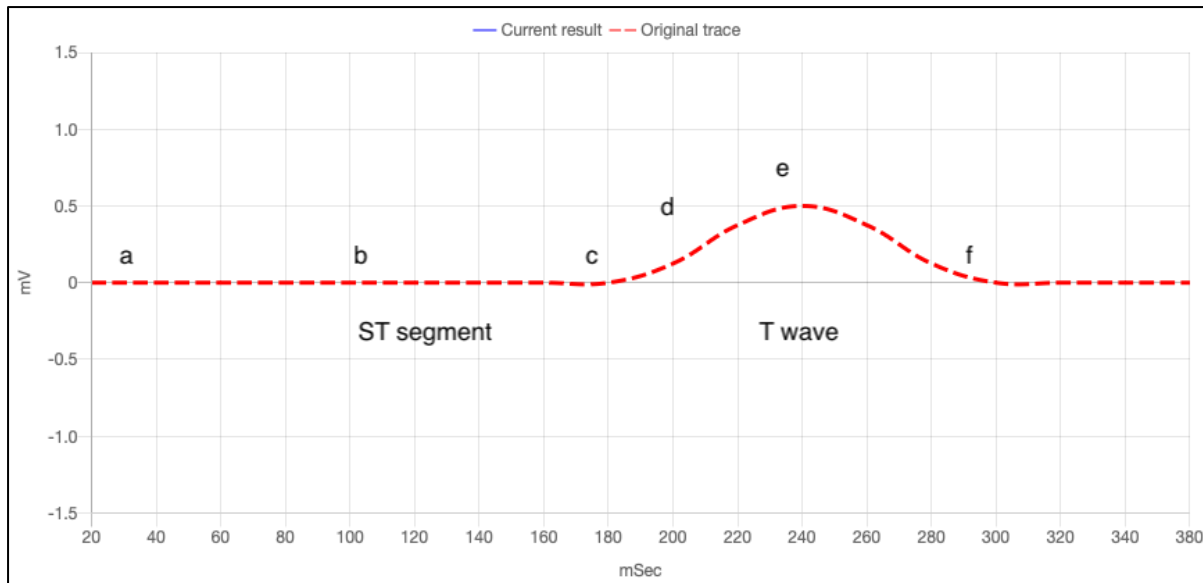
132 The 'components' in this model consist of the signal itself, any enhancement of the
133 signal caused by hypertrophy, and any damage in the muscle mass (location and
134 severity).

135 As demonstrated in Figure 3, initially the positive and negative deflections in that lead
136 balance out yielding a net isoelectric reading until the asymmetrical part of the egg
137 shape is reached. This is the ST segment (Figures 3a to 3c). When the signal reaches the
138 asymmetrical part of the egg shape, termed as the 'T-zone', an excess signal on one side
139 which causes a deflection in the lead trace. In Figure 3d, this results in a rising positive
140 deflection, which peaks when the signal's front edge reaches the outer boundary of the
141 'T-zone' (Figure 3e). Eventually the repolarisation signal works its way out of the 'T-zone'
142 of the egg shape (asymmetrical part) causing the positive deflection in the lead to return
143 to the isoelectric line (Figure 3f). Once the signal has exited, the entire shape has
144 become repolarised, ready for the next signal.



145

146 **Figure 3: The repolarisation sequence of the heart.** These diagrams show the progression of an
147 expanding repolarisation wave from the WCT within the egg-shaped heart. The 'T-zone' refers to the
148 asymmetric region of the egg shape, crucial in generating the T-wave in this lead.



149

150 **Figure 4: The ECG trace produced by repolarisation.** This graph displays the ECG trace generated by the
151 expanding repolarisation signal in the Simplified Egg and Changing Yolk Model. The letters correspond to
152 the signal's position in Figures 3a to 3f.

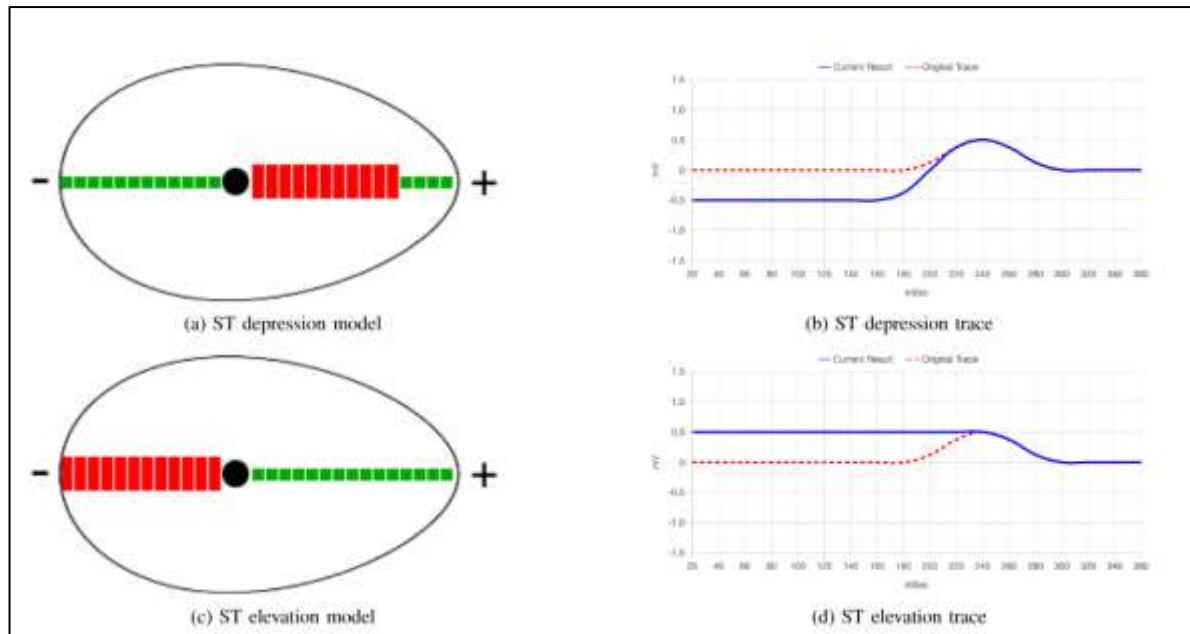
153 From the repolarisation sequence (shown in Figure 3) and the corresponding net
154 deflections in Figure 4, the ECG trace stays on the isoelectric line (balanced) during the
155 ST interval. A net positive signal is detected on the lead only when the repolarisation
156 signal enters the asymmetrical portion of the egg shape (T-zone) and continues until the
157 signal exits this boundary. In the proposed model, this 'T-zone' is responsible for
158 generating the T-wave observed in the ECG. The time from the onset of repolarisation to
159 the stage when the signal reaches the boundary of the 'T-zone' (Figures 3a to 3e)
160 corresponds to the Q-wave start to T-wave peak (QTp) interval. In contrast, the
161 commonly used corrected QT interval (QTc) spans from the start of the Q-wave to the
162 point when the repolarisation signal has propagated out of the 'T-zone' (from 3a to 3f in
163 the sequence). The QTp interval is marked when the repolarisation signal reaches the 'T-
164 zone' boundary, while the QTc interval indicates when the signal exits the boundary.

165 Comparing the QTc and QTp intervals, the QTp is more clearly defined and more reliably
166 calculable.

167 Model Repolarisation Patterns with Heart Damaged Areas

168 The Simplified Egg and Changing Yolk Model offers a framework for studying the effects
169 of damage to specific regions of heart that no longer contributes a repolarisation signal
170 through the electrically inert area. In Figures 5a and 5c, the red areas represent where
171 along the lead the damage, or non-electrical regions, are registered.

172 In Figure 5a, as the repolarisation signal spreads, there is a deficit of positive deflection
173 and this results in ST depression because the signal seems to be moving away from the
174 lead overall. Since the damage is close to the WCT, the ST depression occurs right from
175 the start of repolarisation. If the damaged region of the heart is situated at a greater
176 distance from the WCT, the resulting ST depression will manifest later. Consequently,
177 the onset of ST depression signifies the location of damage relative to the WCT and the
178 direction of the lead. In Figure 5c, the damage is on the opposite side of the WCT, which
179 results in ST elevation in this case because of the lack of transmission in negative
180 deflection.

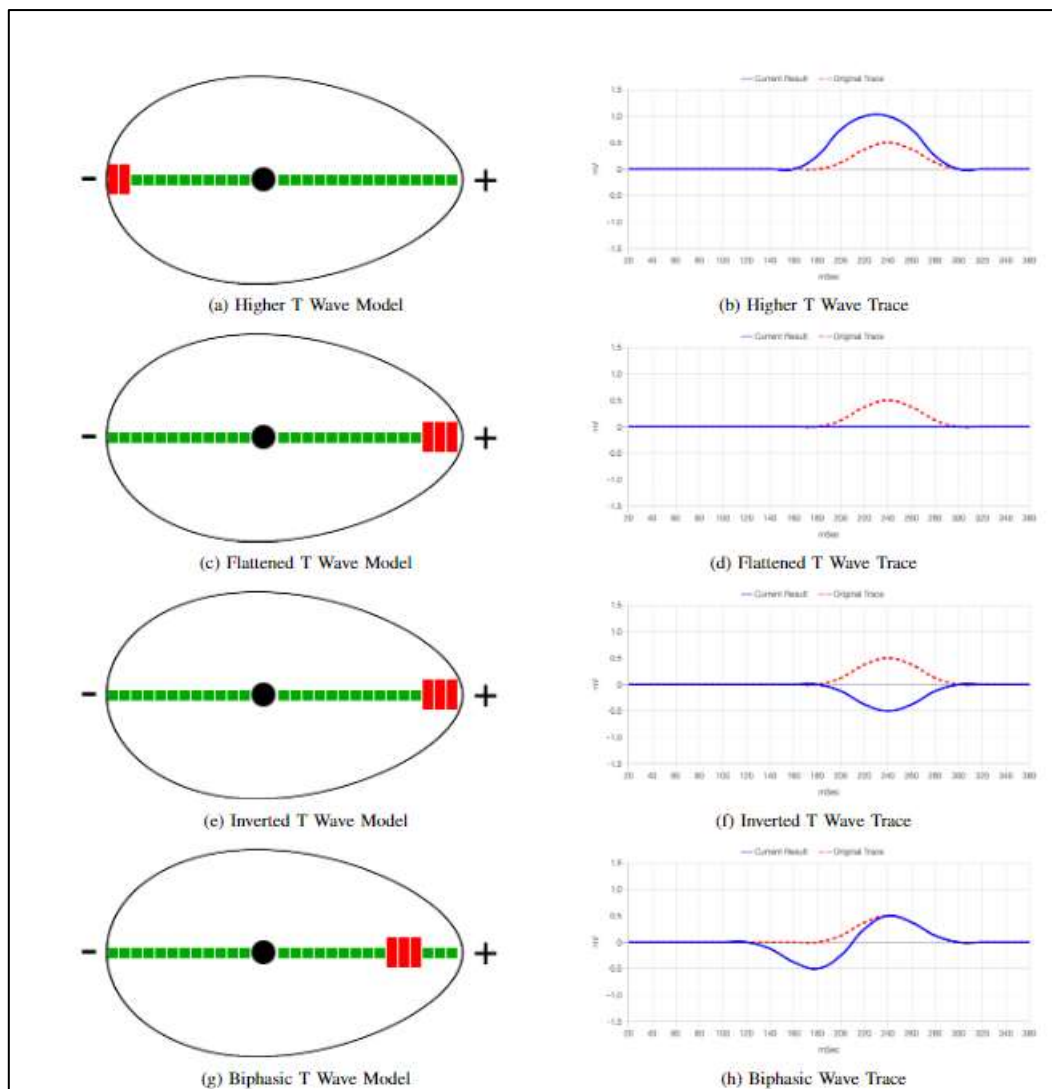


181

182 **Figure 5: ST depression and ST elevation models and traces.** The diagrams illustrate how ST depression
183 and ST elevation traces on an ECG can result from the Simplified Egg and Changing Yolk Model.

184 The proposed model can also be used to investigate other abnormal T-wave
185 morphologies. The sequence in Figure 6 represents the regions on the lead which
186 register the damaged areas and their resulting traces. They depict the commonly seen
187 abnormal T-wave morphologies of higher T-waves, flattened T-waves, inverted T-waves,
188 and biphasic T-waves along with drawings of their registered damaged areas within the
189 egg shape.

190 In Figure 6a, the higher T-wave is depicted as resulting from muscle damage on the
191 negative side of the WCT for the lead. However, other factors such as hypertrophy and
192 ion imbalance, can also produce higher T-waves. Note that while the settings for the
193 flattened and inverted T-waves (Figures 6c and 6e) seem similar, they differ in
194 hypertrophy and damage severity to reproduce the T-wave morphologies. Further
195 details on these examples can be explored using the webtool available at: [https://t-](https://t-wave.aber.ac.uk/)
196 [wave.aber.ac.uk/](https://t-wave.aber.ac.uk/)



197

198 **Figure 6: Representation of Abnormal T-wave Morphologies on ECG Traces.** These diagrams
199 demonstrate how the Simplified Egg and Changing Yolk Model can reproduce four common abnormal T-
200 wave morphologies on an ECG by placing damaged registered areas (red blocks) in specific parts of the
201 egg shape.

202 A comprehensive range of T-wave shapes, along with corresponding real-world ECG
203 examples can illustrate how this simple, yet versatile model can emulate various real-
204 life T-wave abnormalities and explain the presence of three distinct T-wave shapes
205 (positive, biphasic, and inverted) following ST depression, compared to the single T-
206 wave shape (positive) observed after ST elevation in lead V5. The proposed model also
207 demonstrates how the model can account for variations in T-wave shapes in 'normal

208 ECGs', depending on the orientation and shape of the heart relative to lead direction
209 (see Supplementary Material section 2).

210

211 **Discussion**

212 We have demonstrated that the novel Simplified Egg and Changing Yolk Model is a
213 multifaceted model for illustrating the conditions that give rise to various T-wave
214 morphologies in ECG traces. The proposed model specifically applies to the
215 repolarisation process, with the T-wave representing ventricular repolarisation. Since
216 ventricular depolarisation travels quickly through cardiac nerve fibres, like the bundle of
217 His, bundle branches, and Purkinje fibres, necessitating a different model. In contrast,
218 the ventricular repolarisation process, which resets the depolarised ventricular
219 muscles, is not facilitated by these nerve fibres, making the Simplified Egg and
220 Changing Yolk Model suitable for replicating this process. While the examples used lead
221 V5, these principles apply to other ECG leads as well. However, the orientation of each
222 lead within the 'egg shape' must be considered. Lead V5 was chosen for demonstration
223 due to its alignment with the heart apex, matching the most asymmetric part of the 'egg
224 shape'.

225 The implications of this model of ventricular repolarisation challenges the conventional
226 view that the repolarisation process commences only at the conclusion of the S wave.
227 Instead, it suggests repolarisation starts with the Q-wave as depolarisation begins and
228 continues as a single process through to the end of the T-wave. Consequently, the ST
229 interval and T-wave interval should be considered as a unified process, rather than

230 being divided into separate components as is currently believed¹⁶. Secondly, given that
231 ST depression in one lead manifests as ST elevation in its reciprocal lead, it becomes
232 difficult to reliably interpret ST depression as indicative of myocardial ischaemia or ST
233 elevation as representative of myocardial infarction¹⁷. Using this model, it is more
234 appropriate to consider the entire repolarisation process as a single unit and attempt to
235 determine ‘where’ the myocardial issue is occurring (rather than focusing on ‘what’ is
236 happening). Other investigative methods, such as cardiac enzyme analysis, should be
237 used as markers for potential myocardial damage. Thirdly, there are implications for use
238 of the QTc interval. Currently the QTc interval ends when repolarisation exits the ‘T-zone’
239 of the Simplified Egg and Changing Yolk Model. This approach uses the ‘front’ of the
240 wave of the repolarisation signal (Q-wave start) and the ‘tail end’ of the wave of the
241 repolarisation signal when it exits the ‘T-zone’. In practice, challenges arise in
242 calculating the QTc interval when a U-wave appears before the T-wave ends or when a
243 P-wave begins before the T-wave concludes. For examples of these challenges in QTc
244 calculation, please refer to Supplementary Material section 1.

245 There is no universally accepted formula for calculating the QTc interval. Multiple
246 recognised formulae exist, each with advantages and limitations, leading to potential
247 discrepancies in clinical practice¹⁸. The most commonly used are Bazett’s, Fridericia’s,
248 Hodges’ and Framingham’s formulae. The choice of the most appropriate formula
249 should be carefully considered based on the clinical context and population studied¹⁹.

250 The proposed model suggests measuring the interval from the onset of the Q-wave up
251 to the T-wave peak, termed the QTp interval. This interval represents the duration from
252 the start of repolarisation at the Q-wave to the outer boundary of the ‘T-zone’ at the T-
253 wave peak. Measuring the QTp interval reduces ambiguity in the QT interval

254 measurement and simplifies the automated detection of the T-wave peak. This is
255 contrary to calculating the T-wave end based on the different formulae used by the ECG
256 machine and this approach is supported by multiple studies²⁰⁻²². For biphasic T-waves,
257 the highest T-wave peak should be used, and for inverted T-waves the lowest trough
258 position is used. However, in cases of flat T-waves, neither the QTp nor the QTc interval
259 can be determined. The proposed model lends stronger support to the case for using
260 the QTp interval as a more reliable and accurate parameter, especially in assessing the
261 risk of arrhythmia caused by potential 'R on T phenomenon', and in measuring the
262 effects of medication on the QT interval²³⁻²⁵.

263 Finally, the Simplified Egg and Changing Yolk Model can be used to reproduce various
264 ECG abnormalities, including ST elevation, ST depression and T-wave flattening or
265 inversion. By selecting multiple blocks to simulate "damage" in the model, one can
266 reflect the distribution of the affected artery. Future investigations could modify the
267 model to incorporate coronary artery distribution, aiming to replicate the effects of
268 occlusion in specific arteries.

269 **Conclusion**

270 In conclusion, this study introduces the Simplified Egg and Changing Yolk Model, a
271 comprehensive framework that enhances our understanding of T-wave morphologies
272 on ECGs during ventricular repolarisation. By offering a unified model that explains
273 various T-wave patterns, this work could improve ECG interpretation and lead to more
274 accurate diagnoses of cardiac abnormalities.

275 Furthermore, the proposed model underscores the limitations of the widely used QTc
276 interval in assessing arrhythmia risk and supports the QTp interval as a more reliable

277 alternative. By demonstrating the QTp interval's effectiveness in evaluating arrhythmia
278 risk and the impact of QT-prolonging medications, this model offers a valuable tool for
279 improving risk stratification and patient management in cardiac diseases. We
280 recommend adopting the more reliable QTp (Q-wave start to T-wave peak) interval over
281 the QTc interval, especially for assessing medication effects on the QT interval.

282 Our work has important implications for clinical practice and research, offering a better
283 understanding of ventricular repolarisation on ECGs. This can improve decision-making
284 in patient management and aid in developing new therapeutic strategies. Our
285 recommendation for the QTp interval paves the way for future research to validate its
286 utility across different populations and settings and to refine the Simplified Egg and
287 Changing Yolk Model. This study represents a significant step toward improving the
288 assessment and management of cardiac conditions, with the potential to enhance
289 patient outcomes and overall cardiovascular health.

290 Building on this work, we plan to explore the ventricular repolarisation signal's
291 behaviour as it propagates beyond the T-zone within the egg shape, potentially
292 uncovering the origin of the U-wave. We also aim to apply this model to the atrial
293 repolarisation process and explore its broader implications. By expanding our insights,
294 we can advance understanding in cardiac electrophysiology, leading to improved
295 patient care and outcomes.

296 **References**

- 297 1. Kaplan Berkaya S, Uysal AK, Sora Gunal E, Ergin S, Gunal S, Gulmezoglu MB: A
298 survey on ECG analysis. Biomedical Signal Processing and Control 2018; 43:216–
299 235.

- 300 2. Kligfield P, Gettes LS, Bailey JJ, et al.: Recommendations for the Standardization
301 and Interpretation of the Electrocardiogram: Part I: The Electrocardiogram and Its
302 Technology: A Scientific Statement From the American Heart Association
303 Electrocardiography and Arrhythmias Committee, Council on Clinical Cardiology;
304 the American College of Cardiology Foundation; and the Heart Rhythm Society
305 *Endorsed by the International Society for Computerized Electrocardiology*.
306 *Circulation* 2007; 115:1306–1324.
- 307 3. Nielsen JC, Lin Y-J, De Oliveira Figueiredo MJ, et al.: European Heart Rhythm
308 Association (EHRA)/Heart Rhythm Society (HRS)/Asia Pacific Heart Rhythm Society
309 (APHRS)/Latin American Heart Rhythm Society (LAHRS) expert consensus on risk
310 assessment in cardiac arrhythmias: use the right tool for the right outcome, in the
311 right population. *EP Europace* 2020; 22:1147–1148.
- 312 4. Hammad M, Maher A, Wang K, Jiang F, Amrani M: Detection of abnormal heart
313 conditions based on characteristics of ECG signals. *Measurement* 2018; 125:634–
314 644.
- 315 5. Savonitto S: Prognostic Value of the Admission Electrocardiogram in Acute
316 Coronary Syndromes. *JAMA* 1999; 281:707.
- 317 6. Katz AM: T Wave “Memory”: Possible Causal Relationship to Stress-Induced
318 Changes in Cardiac Ion Channels? *Cardiovasc electrophysiol* 1992; 3:150–159.
- 319 7. Cardona A, Zareba KM, Nagaraja HN, et al.: T-Wave Abnormality as
320 Electrocardiographic Signature of Myocardial Edema in Non-ST-Elevation Acute
321 Coronary Syndromes. *JAHA* 2018; 7:e007118.
- 322 8. Klabunde RE: *Cardiovascular physiology concepts*. 2. ed. Philadelphia: Wolters
323 Kluwer [u.a.], 2012,.
- 324 9. Sagie A, Larson MG, Goldberg RJ, Bengtson JR, Levy D: An improved method for
325 adjusting the QT interval for heart rate (the Framingham Heart Study). *The*
326 *American Journal of Cardiology* 1992; 70:797–801.
- 327 10. Goldenberg I, Moss AJ, Zareba W: QT Interval: How to Measure It and What Is
328 “Normal.” *Cardiovasc electrophysiol* 2006; 17:333–336.
- 329 11. Panikkath R, Reinier K, Uy-Evanado A, et al.: Prolonged Tpeak-to-Tend Interval on
330 the Resting ECG Is Associated With Increased Risk of Sudden Cardiac Death. *Circ*:
331 *Arrhythmia and Electrophysiology* 2011; 4:441–447.
- 332 12. Al-Khatib SM, LaPointe NMA, Kramer JM, Califf RM: What Clinicians Should Know
333 About the QT Interval. *JAMA [Internet]* 2003 [cited 2024 Dec 10]; 289. Available
334 from: <http://jama.jamanetwork.com/article.aspx?doi=10.1001/jama.289.16.2120>
- 335 13. Giudicessi JR, Noseworthy PA, Ackerman MJ: The QT Interval: An Emerging Vital
336 Sign for the Precision Medicine Era? *Circulation* 2019; 139:2711–2713.

- 337 14. Wilson FN, MacLeod AG, Barker PS: The T deflection of the electrocardiogram.
338 Trans Assoc Am Physicians 46:29–38.
- 339 15. Meijborg VMF, Conrath CE, Opthof T, Belterman CNW, De Bakker JMT, Coronel R:
340 Electrocardiographic T Wave and its Relation With Ventricular Repolarization Along
341 Major Anatomical Axes. *Circ: Arrhythmia and Electrophysiology* 2014; 7:524–531.
- 342 16. Goldberger AL, Shvilkin A, Goldberger ZD, Goldberger AL: Goldberger’s clinical
343 electrocardiography: a simplified approach. Ninth Edition. Philadelphia, PA:
344 Elsevier, 2017,.
- 345 17. Pollehn T, Brady WJ, Perron AD, Morris F: The electrocardiographic differential
346 diagnosis of ST segment depression. *Emergency Medicine Journal* 2002; 19:129–
347 135.
- 348 18. Vandenberk B, Vandael E, Robyns T, et al.: Which QT Correction Formulae to Use
349 for QT Monitoring? *JAHA* 2016; 5:e003264.
- 350 19. Suárez-León AA, Varon C, Willems R, Van Huffel S, Vázquez-Seisdedos CR: T-wave
351 end detection using neural networks and Support Vector Machines. *Computers in*
352 *Biology and Medicine* 2018; 96:116–127.
- 353 20. Madeiro JPV, Nicolson WB, Cortez PC, et al.: New approach for T-wave peak
354 detection and T-wave end location in 12-lead paced ECG signals based on a
355 mathematical model. *Medical Engineering & Physics* 2013; 35:1105–1115.
- 356 21. Schläpfer J, Wellens HJ: Computer-Interpreted Electrocardiograms. *Journal of the*
357 *American College of Cardiology* 2017; 70:1183–1192.
- 358 22. Postema P, Wilde A: The Measurement of the QT Interval. *CCR* 2014; 10:287–294.
- 359 23. Liu MB, Vandersickel N, Panfilov AV, Qu Z: R-From-T as a Common Mechanism of
360 Arrhythmia Initiation in Long QT Syndromes. *Circ: Arrhythmia and*
361 *Electrophysiology* 2019; 12:e007571.
- 362 24. Sundqvist K, Sylvén C: Cardiac repolarization properties during standardized
363 exercise test as studied by QT, QT peak and terminated T-wave intervals. *Clinical*
364 *Physiology* 1989; 9:419–425.
- 365 25. Haapalahti P, Viitasalo M, Perhonen M, et al.: Comparison of QT peak and QT end
366 interval responses to autonomic adaptation in asymptomatic LQT1 mutation
367 carriers: QT peak versus QT end responses in LQT1. *Clinical Physiology and*
368 *Functional Imaging* 2011; 31:209–214.

369